On the indoor hygrothermal regulation ability of earth building walls

Leonardo Maria Lalicata[1,*], *Agostino Walter* Bruno[1], and *Domenico* Gallipoli[1]

[1]University of Genova, Department of Civil Environmental and Chemical Engineering, via Montallegro, 1 16145 Genova, Italy

Abstract. A coupled finite element model has been developed to investigate the ability of earth walls to regulate indoor hygrothermal conditions. The model simulates heat and water transfers across earth walls, accounting for pore water phase changes and the associated latent heat fluxes. The constitutive laws adopted in this study are grounded in the thermodynamics of porous media and the mechanics of unsaturated soils. All the hygrothermal properties of the earth are expressed as functions of material porosity and water retention characteristics. Therefore, the hygrothermal response of earth walls is fully described by only six parameters, which greatly simplifies sensitivity analyses. The model has been used to explore the effects of latent heat fluxes on the evolution of moisture and temperature inside an idealised room enclosed by two infinite earth walls. In the absence of indoor heat and moisture sinks or sources, the results demonstrate that latent heat buffering intensifies with increasing relative humidity gradients between outdoor and indoor environments. For instance, during cold and humid winters, vapour condenses in the colder outer layers of the wall, generating a local peak in latent heat flux. The condensed moisture then migrates inward toward the warmer core of the wall, where it re-evaporates, thus promoting further condensation at the outer surface. The overall latent heat exchange, which is governed by these hygroscopic processes, becomes more pronounced in walls with higher porosity, steeper retention curves and greater saturation levels.

1 Introduction

Earth has gained popularity as a sustainable building material due to its lower environmental impact compared to conventional alternatives like concrete and fired bricks [1], [2], [3]. Earthen materials act as effective passive hygrothermal regulators, enhancing indoor comfort and reducing air conditioning demands. While some research has explored latent heat buffering by pore water on hygrothermal comfort [4], more attention has been given to incorporating energy-intensive phase change materials in building structures [5]. As a result, natural heat exchanges due to pore water evaporation and condensation in earthen materials remain partially unexploited.

To address this gap, the research group at the University of Genova developed a hygrothermal model integrating unsaturated soil theories with the thermodynamics of porous media [6], [7], [8], [9]. Unlike traditional models, their approach requires fewer parameters while capturing the effects of phase changes and latent heat fluxes on the hygrothermal behaviour of earth materials. Their findings highlight that the moisture buffering value (MBV) of earth is primarily influenced by unsaturated permeability and moisture storage sensitivity to relative humidity. However, MBV alone does not fully describe thermal inertia, as latent heat exchanges within the material play a crucial role.

This study presents selected results on the latent heat effects on the hygrothermal comfort and energy efficiency of indoor spaces enclosed by earth walls.

2 Hygrothermal model

This study models earth as a rigid three-phase porous medium composed by soil grains, water (liquid and gas), and dry air. It assumes negligible resistance to gas flow, keeping gas pressure equal to atmospheric pressure. The hygrothermal behaviour is analysed by solving coupled balance equations for water mass and thermal energy, as both moisture and heat fluxes depend on relative humidity and temperature gradients. The study omits pore vapour mass changes and suction temperature dependency, as these simplifications maintain accuracy while focusing on key governing terms (see Lalicata et al. [8] for further details).

2.1 Earth state variables

This study adopts the relative humidity h_r and temperature T as the hydraulic and thermal state variables, respectively. These are calculated by simultaneously solving the water mass and energy balance equations introduced in the next section.

The model assumes pure pore water (i.e. zero osmotic potential) and neglects moisture retention hysteresis. Thus, the hydraulic variables, such as the degree of saturation S_l (-), gravimetric water content w_l (-), relative humidity h_r (-), matric suction s (MPa), partial vapour pressure p_v (kPa) or partial vapour density ρ_v (kg/m^3), are uniquely linked to each other by phase

* Corresponding author: leonardo.lalicata@unige.it

equations, constitutive relationships and thermodynamic laws, [9].

The matric suction s (named just suction in the following for simplicity) is the difference between the pore air pressure p_a (MPa) and the pore water pressure p_l (MPa). Because the pore air pressure is assumed atmospheric (i.e. $p_a = 0$), the suction s coincides with the pore water pressure p_l changed of sign. The suction s is related to the degree of saturation S_l through the water retention relationship. This work adopts the Van Genuchten [10] water retention relationship:

$$S_l = S_{res} + \left(1 - S_{res}\right) S_e \tag{1a}$$

where S_{res} is the residual degree of saturation while S_e is the effective degree of saturation defined as:

$$S_e = \left(1+\left(s/P\right)^N\right)^{-M} \tag{1b}$$

where P (MPa) and N (-) are independent model parameters, while and M (-) is set equal to *1 - 1/N*.

At a given temperature T (K) and in the absence of osmotic effects, the suction s is linked to the relative humidity h_r by the Kelvin's equation:

$$s = -\rho_l \frac{R}{M_w} T\, ln\left(h_r\right) \tag{2}$$

where ρ_l (1000 kg/m^3) is the liquid water density, R (8.314 J/(mol K)) is the perfect gas constant and M_w (0.018 kg/mol) is the molar mass of water.

2.2 Governing balance equations

Under standard service conditions, the moisture flow across building walls is mostly horizontal and the pore water pressure gradient governs liquid transfer according to Darcy law, while the contribution of the gravitational gradient is negligible. Under this hypothesis, and assuming vapour storage is negligible, the water mass balance and the thermal energy balance equations are given by:

$$C_l \frac{\partial h_r}{\partial t} = \nabla\left(\begin{array}{l} D_l \rho_l \nabla h_r + \\ +\left(D_v \frac{M_w}{RT}\left(\begin{array}{l} p_{sat}\nabla h_r + \\ -h_r\left(\frac{dp_{sat}}{dT} - \frac{p_{sat}}{T}\right)\nabla T \end{array}\right)\right) \end{array}\right) \tag{3}$$

$$\left(\rho c_p\right)_{eq} \frac{\partial T}{\partial t} = \nabla\left(\lambda \nabla T\right) + L_v\left(C_l \frac{\partial h_r}{\partial t} - \nabla\left(D_l \rho_l \nabla h_r\right)\right) \tag{4}$$

where C_l (kg/m^3) is the volumetric liquid water capacity:

$$C_l = \rho_l n \frac{\partial S_l}{\partial h_r} \tag{5}$$

where n is the porosity. D_l (m^2/s) is the liquid water diffusivity:

$$D_l = \frac{K_l}{g} \frac{R}{M_w} \frac{T}{h_r} \tag{6}$$

And D_v (m^2/s) is the vapour diffusivity:

$$D_v = D\tau n\left(1 - S_l\right) \tag{7}$$

where τ (-) is the tortuosity tensor, which is assumed isotropic and coincident with the following scalar quantity as in [11]:

$$\tau = \left(n\left(1 - S_l\right)\right)^{2/3} \tag{8a}$$

while the vapour diffusivity in free air D (m^2/s) depends on the temperature T (K):

$$D = 0.229 \cdot 10^{-4}\left[1 + \frac{T}{273}\right]^{1.75} \tag{7b}$$

In eq. (6) the unsaturated permeability K_l (m/s) is defined as:

$$K_l = K_{sat} k_{rl} \tag{9}$$

where k_{rl} (-) is the relative permeability function of the effective degree of saturation S_e:

$$k_{rl} = \sqrt{S_e}\left[1 - \left(1 - S_e^{1/M}\right)^M\right]^2 \tag{10a}$$

where M is the same parameter as in the Van Genuchten relationship of eq. (1b). The saturated permeability K_{sat} (m/s) depends on porosity n according to the power relationship of Ren *et al.* (2016):

$$K_{sat} = 10^{\left(3.2\frac{n}{1-n} - 7\right)} \tag{10b}$$

In the thermal balance of eq. (4), the volumetric heat capacity of the soil $\left(\rho c_p\right)_{eq}$ kJ/(m^3·K)) is calculated by averaging the contributions of the solid and liquid phases as:

$$\left(\rho c_p\right)_{eq} = \left(1 - n\right)\rho_s c_{p,s} + n \rho_l c_{p,l} \tag{11}$$

where $c_{p,s}$ and $c_{p,l}$ (kJ/(kg·K)) are the mass heat capacities of solid grains and liquid water, respectively. The values of ρ_s and $c_{p,s}$ vary with soil type while the value of $c_{p,l}$ can be reasonably assumed constant and equal to 4.183 kJ/(kg·K).

The thermal conductivity λ (W/(m·K)) is calculated as a function of both the thermal conductivity of the dry material λ_d and the gravimetric water content w_l [12]:

$$\lambda = \lambda_d + b w_l \tag{12}$$

where b is a model parameter. The dry thermal conductivity λ_d is in turn related to the dry density $\rho_d = \rho_s\left(1 - n\right)$ according to the following empirical relationship by Cagnon *et al.* [13]:

$$\lambda_d = 5.6 \cdot 10^{-2} e^{\left(1.4 \cdot 10^{-3} \rho_d\right)} \tag{13}$$

The last term on the right-hand side of eq. (4) is the latent heat sink/source due to pore water phase changes

and is equal to the product of the water latent heat L_v ($2.5 \cdot 10^6$ J/kg) by the evaporation/condensation rate, which is evaluated from the liquid phase balance as in eq. (3).

2.3 Numerical model

Equations (3) and (4) have been implemented in the Comsol Multiphysics finite element software to calculate the hygrothermal state of an idealised room of width $L_i = 5m$ enclosed by two symmetrical earth walls of thickness $L_w = 0.4m$ (Fig. **1**a), under plain strain conditions.

Due to symmetry reasons, only half geometry is considered, and the problem is modelled as a one-dimensional case. The wall is discretised by a linear mesh while the idealised room is modelled as a single point, assuming spatial uniformity of indoor humidity and temperature (Fig. **1**b). This enables to better focus on the hygrothermal transport across the wall. Therefore, in the absence of indoor sources/sinks of vapour and heat, the relative humidity $h_{r,i}$ and temperature T_i inside the room evolve according to the heat and moisture transfer across the wall. In the room, the moist air relationships have been used to solve the heat and moisture balance equations, further details are given in Lalicata et al. [9].

At the inner and outer boundary, flux conditions have been imposed using standard heat α (W/(m^{2}K)) and vapour mass β (kg/(m^{2}sPa)) transfer coefficients [14]. α is equal to 8 and 23 W/(m^{2}K) at the indoor and outdoor interface, respectively. β is equal to $2.5 \cdot 10^{-8}$ and $7.5 \cdot 10^{-8}$ kg/(m^{2}sPa) at the indoor and outdoor interface, respectively.

The numerical model can thus predict the temporal variation of relative humidity and temperature inside the room according to the imposed external conditions. The reference earth parameters are listed in Table 1.

Wet and cold winter conditions are imposed at the outdoor face by applying constant values of relative humidity and temperature, equal to 0.80 and 8°C, respectively, while the corresponding initial indoor values are 0.50 and 20°C. Initial values of relative humidity and temperature across the wall are identical to those of the indoor environment, i.e. 0.50 and 20°C, respectively.

The results are presented in terms of changes of indoor relative humidity and temperature, calculated over a 50 day period leading to equilibrium with the imposed outdoor conditions. The hygrothermal impact of the pore water phase changes is highlighted by comparing two distinct cases with and without consideration of latent heat, i.e. with $L_v = 2.5 \cdot 10^6$ J/kg and $L_v = 0$, respectively.

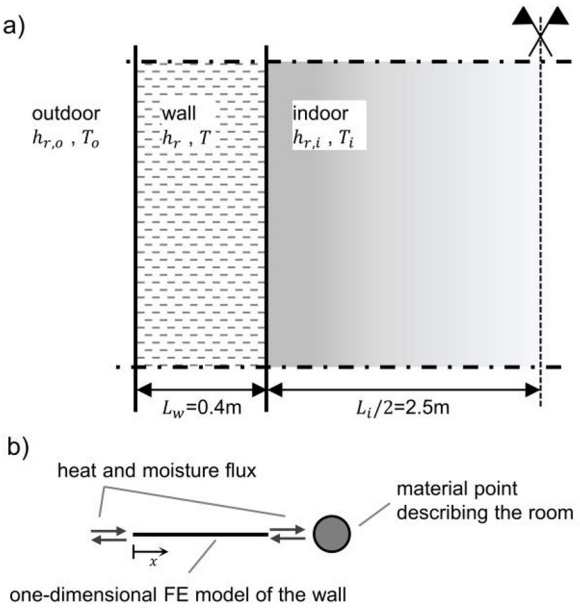

Fig. 1. a) Scheme of symmetric wall-room system (not to scale), b) one-dimensional numerical model.

Table 1. Reference parameter values of earth walls.

Parameter	Symbol	Value
Porosity (-)	n	0.35
Grains density (kg/m^3)	ρ_S	2650
Van Genuchten parameter (MPa)	P	0.9
Van Genuchten parameter (-)	N	1.74
Van Genuchten parameter (-)	M	0.42
Van Genuchten residual saturation (-)	S_{res}	0
Grains heat capacity (kJ/(kgK))	$c_{p,s}$	0.648
Thermal conductivity parameter (W/(mK))	b	9.22

3 Reference Test results

Fig. **2** illustrates that, when latent heat is neglected, the room temperature drops from 20 °C to 8 °C over the first week, reaching thermal equilibrium with the external environment. In contrast, when latent heat is considered, the temperature decreases to 10.5 °C within the same period, then remains stable for around three days before gradually declining to equilibrium at 8 °C. This indicates that the earth's hygrothermal activity mitigates indoor heat loss, maintaining a higher temperature (+2.5 °C) for longer compared to the same material without latent heat.

Unlike temperature, Fig. **2** shows that indoor relative humidity evolves almost identically in both cases. This is because it is primarily governed by hydraulic boundary conditions and remains largely unaffected by latent heat exchanges.

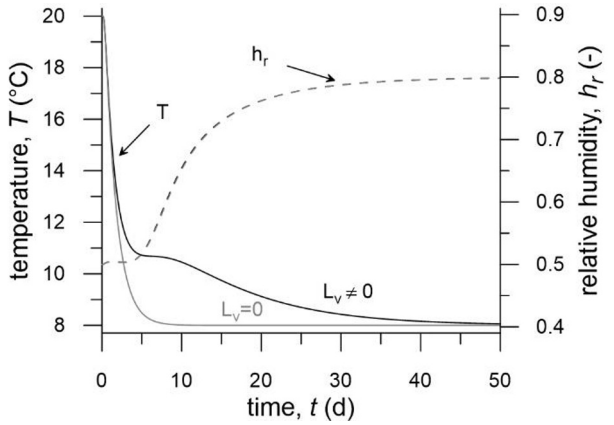

Fig. 2. Influence of pore water latent heat exchanges in earth walls on the evolution of indoor relative humidity and temperature over time.

This beneficial hygrothermal behaviour can be understood by analysing the specific latent heat fluxes (i.e. latent heat fluxes per unit volume) across the wall thickness at different times. As shown in Fig. **3**, the specific latent heat fluxes are highest in the early stages, when the wall hydraulic state is far from equilibrium, leading to significant phase changes of pore water.

Moisture penetration from the outside increases the relative humidity within the earth's pores, exceeding equilibrium with the local pore suction. This imbalance causes water condensation and the subsequent release of latent heat, as indicated by the positive fluxes in Fig. **3**.

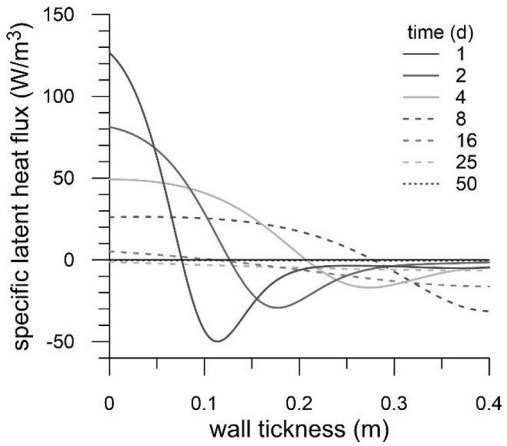

Fig. 3. Distribution of specific latent heat fluxes across the wall core.

However, this heat generation is restricted to the external wall layer due to low gas diffusivity, which limits vapour movement inwards and prevents the condensation front from advancing deeper.

Nevertheless, this restriction is partly counteracted by the inward movement of condensed water, which helps restore pore suction in the external earth layer, along with the potential for further condensation. The condensed water continues moving inward towards the lower humidity regions of the wall, where it reduces local pore suction below equilibrium, triggering evaporation and the absorption of latent heat, as indicated by the negative fluxes in Figure 3.

This ongoing process of condensation followed by liquid transport helps maintaining a relative humidity gradient between the external environment and the earth surface, thus ensuring the continued movement of moisture with the associated latent heat production.

4 Parametric study

Results shown in the previous section have shown the significant impact of the latent heat exchanges during condensation or evaporation of pore water that occur in earth walls. These exchanges grow large when the volumetric liquid water capacity C_l of eq. (5) and the liquid water diffusivity D_l of eq. (6) increase, following the previously described mechanism of condensation and liquid transport. To investigate these effects further, a parametric study has been carried out to explore the sensitivity of indoor hygrothermal conditions to variations in the porosity and water retention properties of earth walls within realistic ranges. Based on the literature [15], [16], the porosity ranges between 0.15 and 0.45, while the changes in the water retention curve are here investigated by varying the parameter N, that governs the slope of the retention curve, between 1.4 and 2.0.

Effect of porosity n

Increasing the porosity produces a beneficial increases of volumetric liquid water capacity C_l, according to eq. (5), and liquid water diffusivity D_l (due to growing saturated permeability K_l), according to eqs. (9) and (10), which result in growing exchanges of latent heat. A larger porosity also produces a beneficial reduction of thermal conductivity λ as the decrease of dry conductivity λ_d outweighs the growth of water content w_l, according to eqs. (12) and (13). On the other hand, an increase in porosity leads to a disadvantageous reduction in volumetric heat capacity $\left(\rho c_p\right)_{eq}$, according to eq. (11).

Finally, it can be demonstrated that that the vapour diffusivity D_v increases with growing porosity one order of magnitude less than the liquid water diffusivity D_l.

Fig. **4** illustrates the temporal evolution of thermal gain ΔT, defined as the difference in indoor temperature between the cases with $L_v \neq 0$ and $L_v = 0$, for different porosity values n, while all other parameters remain fixed at their reference values from Table 1.

For a highly porous material ($n = 0.45$), thermal gain peaks at approximately 7°C after around 4 days, followed by a gradual decline towards zero. In contrast, for a highly compacted material ($n = 0.15$), the hygrothermal performance is significantly lower, with a maximum thermal gain of just 0.2°C, which remains nearly constant throughout the simulation.

Overall, the results in Fig. **4** highlight the threefold benefit of increased porosity: higher volumetric liquid water capacity C_l, greater liquid water diffusivity D_l, and lower thermal conductivity λ. These advantages far

outweigh the negative effect of a reduced equivalent volumetric heat capacity $\left(\rho c_p\right)_{eq}$.

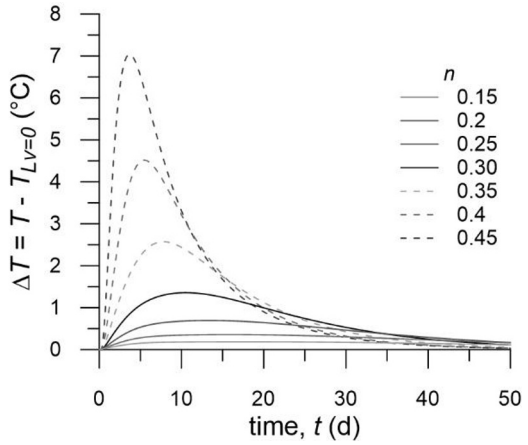

Fig. 4. Thermal gain over time for different values of porosity *n*.

Effect of retention parameter N

The range of N-values represents different retention curves, falling within the limits identified by [16] for relative humidity between 0.3 and 0.8 (equivalent to suction levels from 30 to 170 MPa), typical of building service conditions, as shown in Fig. **5**. A lower N enhances volumetric liquid water capacity C_l, increasing moisture sensitivity to relative humidity eq. (5). It also raises the degree of saturation (eq. (1)), leading to higher liquid water diffusivity D_l (eqs. (9) (10)). These factors promote greater latent heat exchange, as previously discussed. Additionally, higher saturation due to lower N increases volumetric heat capacity $\left(\rho c_p\right)_{eq}$ (eq. (11)), which is beneficial, but also raises thermal conductivity λ, according to eq. (12), which is less desirable. Finally, while liquid water diffusivity D_l varies by three orders of magnitude over this range, vapour diffusivity D_v remains largely unaffected.

Fig. **6** illustrates the evolution of thermal gain ΔT over time for different values of N, while all other parameters remain fixed at their reference values from Table 1. As N decreases from 2.0 to 1.4, the maximum thermal gain rises from 0.2°C to 5.5°C. This increase is attributed to the higher liquid water capacity C_l, liquid water diffusivity D_l, and equivalent volumetric heat capacity $\left(\rho c_p\right)_{eq}$ associated with lower values of N. In contrast, the negative effect of increased thermal conductivity appears to be less significant, at least within the scope of this analysis.

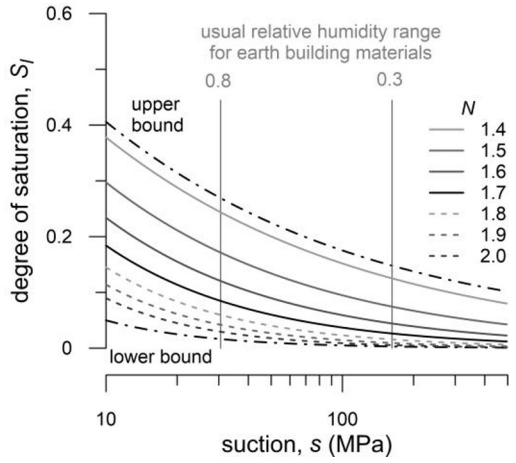

Fig. 5. Water retention curves investigated in this study.

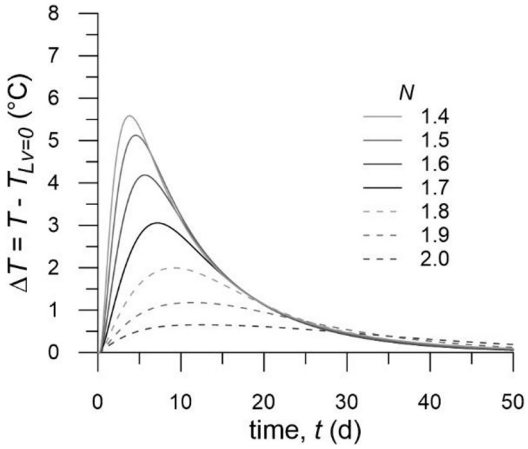

Fig. 6. Thermal gain over time for different values of retention parameter *N*.

Hydraulic effusivity *E*

Results demonstrated that latent heat exchanges in earth walls occur through a condensation and liquid transport mechanism, primarily controlled by the volumetric liquid water capacity C_l and liquid water diffusivity D_l, while vapour diffusivity D_v plays a secondary role. By analogy with thermal processes, hydraulic effusivity E ($\mathrm{kg/m^2\sqrt{s}}$) can be defined as a single parameter governing latent heat exchanges:

$$E = \sqrt{\rho_l D_l C_l} \tag{14}$$

Fig. **7** validates this assumption by showing a strong correlation between the maximum indoor thermal gain ΔT_{max} and the initial hydraulic effusivity E within the earth wall. This correlation holds across two sets of analyses, where porosity *n* and the retention parameter *N* are varied independently while all other parameters remain fixed at their reference values from Table 1. The results suggest that latent heat exchanges play a dominant role in determining ΔT_{max}. However, the divergence between the two curves indicates that additional physical processes, governed by volumetric heat capacity and thermal conductivity – parameters not

included in the definition of hydraulic effusivity – also influence the observed thermal behaviour.

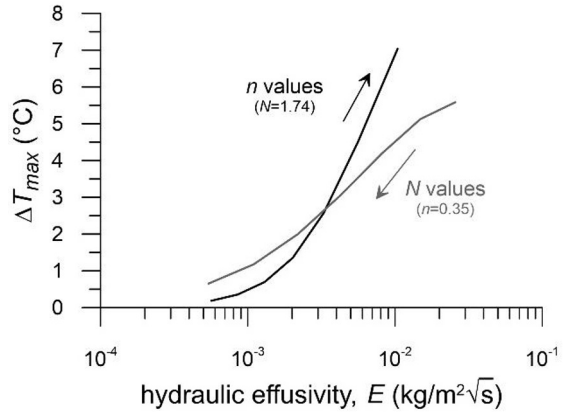

Fig. 7. Maximum thermal gain versus initial hydraulic effusivity *E*.

5 Conclusions

A coupled finite element model has been developed to simulate heat and moisture transfer in earth walls, incorporating pore water phase changes and latent heat fluxes. A simple one-dimensional analysis predicts hygrothermal variations in an idealised room enclosed by two infinitely extended earth walls, exposed to a cold and humid external environment. The model requires only 6 input parameters, as key hygrothermal properties expressed in terms of material porosity and water retention characteristics, enabling efficient parametric studies.

The analysis shows that latent heat buffering increases with greater relative humidity gradients between the moist outdoor air and the drier indoor space. Due to low vapour diffusivity, condensation and latent heat production occur mainly in the colder outer wall regions, where pore vapour condenses. The condensed moisture then migrates inward in liquid form before evaporating back into the pore space.

The effectiveness of this process is enhanced when the volumetric capacity and diffusivity of liquid water are high. Volumetric capacity increases with porosity and the steepness of the retention curve, while diffusivity rises with higher permeability, which itself depends on porosity and degree of saturation. Consequently, highly porous walls with strong moisture sensitivity and generally high saturation levels maximise latent heat exchanges. However, these characteristics may conflict with structural requirements for compact and relatively dry perimeter walls, necessitating a careful balance in design.

Similar to thermal processes, hydraulic effusivity, defined as a function of both the volumetric capacity and diffusivity of liquid water, serves as a key parameter governing latent heat exchanges. Higher hydraulic effusivity indicates greater potential for latent heat buffering.

References

[1] A. E. Losini, A.-C. Grillet, L. Vo, G. Dotelli, M. Woloszyn. Build. Environ. **233**, 110087 (2023). doi: 10.1016/j.buildenv.2023.110087.
[2] J. M. F. Pardo. Buildings. **13**, 162 (2023). doi: 10.3390/buildings13010162.
[3] A. W. Bruno, L. M. Lalicata, R. Abdallah, A. Lagazzo, S. Arris-Roucan, F. McGregor, C. Perlot, D. Gallipoli. Constr. Build. Mater., **439**, 137258 (2024). doi: 10.1016/j.conbuildmat.2024.137258.
[4] L. Ben-Alon, A. R. Rempel. Build. Environ. **238**, 110339 (2023). doi: 10.1016/j.buildenv.2023.110339.
[5] C. Mankel, A. Caggiano, N. Ukrainczyk, E. Koenders. Constr. Build. Mater. **199**, 307–320 (2019). doi: 10.1016/j.conbuildmat.2018.11.195.
[6] L. M. Lalicata, A. W. Bruno, D. Gallipoli. *Geotechnical Engineering in the Digital and Technological Innovation Era*. (2023), 327–334. doi: 10.1007/978-3-031-34761-0_40.
[7] L. M. Lalicata, A. W. Bruno, D. Gallipoli. *E3S Web Conf.* **382**, 23003 (2023). doi: 10.1051/e3sconf/202338223003.
[8] L. M. Lalicata, A. W. Bruno, D. Gallipoli. It. Geotech J. **1275**, 11–24 (2024). doi: 10.19199/2024.1.0557-1405.011.
[9] L. M. Lalicata, A. W. Bruno, D. Gallipoli. Energy Build. **328**, 115163 (2025). doi: 10.1016/j.enbuild.2024.115163.
[10] M. Th. van Genuchten. Soil Sci. Soc. Am. J. **44**, 892–898 (1980). doi: 10.2136/sssaj1980.03615995004400050002x.
[11] S.H. Lai, J.M. Tiedje, A.E. Erickson. Soil Sci. Soc. Am. J. **40**, 3-6 (1976).
[12] A. E. Losini, T. Chitimbo, L. Létévé, M. Woloszyn, A.-C. Grillet, N. Prime. E3S Web Conf. **382**, 23004 (2023). doi: 10.1051/e3sconf/202338223004.
[13] H. Cagnon, J. E. Aubert, M. Coutand, C. Magniont. Energy Build. **80**, 208–217 (2014). doi: 10.1016/j.enbuild.2014.05.024.
[14] H. M. Künzel. **65** (1995).
[15] G. Giuffrida, R. Caponetto, F. Nocera. *Sustainability*, **11**, 5342 (2019). doi: 10.3390/su11195342.
[16] D. Gallipoli, A. W. Bruno, C. Perlot, J. Mendes. Acta Geotech., **12**, 463–478 (2017). doi: 10.1007/s11440-016-0521-1.